

***CloudSat* Studies of Stratiform Precipitation Systems Observed in the Vicinity of the Southern Great Plains Atmospheric Radiation Measurement Site**

SERGEY Y. MATROSOV

Cooperative Institute for Research in Environmental Sciences, University of Colorado, and NOAA/Earth System Research Laboratory, Boulder, Colorado

(Manuscript received 3 December 2009, in final form 1 March 2010)

ABSTRACT

The spaceborne W-band (94 GHz) radar on board the *CloudSat* polar-orbiting satellite offers new opportunities for retrieving parameters of precipitating cloud systems. *CloudSat* measurements can resolve the vertical cross sections of such systems. The radar brightband features, which are commonly present when observing stratiform precipitating systems, allow the vertical separation of the ice, mixed, and liquid precipitating hydrometeor layers. In this study, the *CloudSat* data are used to simultaneously retrieve ice water path (IWP) values for ice layers of precipitating systems using absolute radar reflectivity measurements and mean rainfall rates R_m in the liquid hydrometeor layers using the attenuation-based reflectivity gradient method. The retrievals were performed for precipitating events observed in the vicinity of the Southern Great Plains (SGP) Atmospheric Radiation Measurement Program (ARM) Climate Research Facility. The retrieval results indicated that IWP values in stratiform precipitating systems vary from a few hundreds up to about 10 thousands of grams per meter squared, and the mean rain rates were in a general range between 0.5 and about 12 mm h⁻¹. On average, mean rainfall increases with an increase in ice mass observed above the melting layer; the corresponding mean correlation coefficient is about 0.35, although events with higher correlation as well as those with no appreciable correlation were observed. Horizontal advection, wind shear, and vertical air motions might be some of the reasons for decorrelation between IWP and R_m retrieved for the same vertical atmospheric column. A mean statistical relation between IWP and R_m derived from *CloudSat* retrievals is in good agreement with the data obtained from multiwavelength ground-based cloud radar measurements at the SGP site.

1. Introduction

The first spaceborne W-band (94 GHz) cloud-profiling radar (CPR) (e.g., Tanelli et al. 2008) on board the *CloudSat* satellite launched in spring 2006 provides new opportunities for quantitative estimations of ice and rainfall parameters in precipitating cloud systems. The first years of *CloudSat* operations have yielded unique global information on occurrence and microphysical and macrophysical properties of nonprecipitating clouds (e.g., Stephens et al. 2008). While providing quantitative information about such clouds is the main scientific objective of the *CloudSat* project, the CPR also has proved to be a very valuable tool for studies of rainfall and thick precipitating clouds.

The W-band frequencies are the highest operationally used in radar remote sensing of the atmosphere. Signals

at these frequencies experience strong attenuation by liquid hydrometeors. Despite this attenuation, the CPR is often able to “see” through precipitating cloud systems and detect attenuated ground returns during lighter rainfall events. For such events, the path-integrated attenuation (PIA) approach was devised to estimate mean layer rain rate over water surfaces in stratiform rainfall (Haynes et al. 2009). Another method for *CloudSat* rainfall retrievals is based on relating the height derivatives of observed CPR reflectivity factors Z_e (hereinafter just reflectivities) to rain rate (Matrosov 2007). This approach does not require the presence of surface returns and can be applied to retrievals of light-to-moderate rainfalls above both water and land surfaces.

Because of a relatively high sensitivity (~-28 dBZ) and low signal attenuation in the ice cloud phase, the CPR is able to observe the full vertical extent of thick ice regions of precipitating systems with tops that can reach altitudes of 16 km or so. Radar backscatter from rainfall parts of such systems (especially lower regions) is usually strongly attenuated and there are significant contributions

Corresponding author address: Sergey Y. Matrosov, R/PSD2, 325 Broadway, Boulder, CO 80305.
E-mail: sergey.matrosov@noaa.gov

to measured CPR returns from multiple scattering effects (e.g., Battaglia et al. 2008). Unlike ground-based W-band radar measurements, multiple scattering effects can noticeably enhance *CloudSat* reflectivities from rainfall because of a relatively large CPR footprint of about 1.5 km. These effects should be accounted for in *CloudSat*-based quantitative rainfall retrievals. The ability of the CPR to provide valuable information about precipitation has been realized by the *CloudSat* community and even some preliminary hurricane studies using CPR measurements have been performed (e.g., Durden et al. 2009).

This study presents results of simultaneous retrievals of hydrometeor parameters of rainfall and ice regions of stratiform precipitating systems over land. These parameters include the mean rain rate in the liquid hydrometeor layer and the integrated amount of ice located above the melting layer. Both rainfall and ice cloud retrievals correspond to the same vertical atmospheric column as resolved by the nadir-looking CPR. The *CloudSat* precipitating cloud system retrievals presented and analyzed in this study were performed for events observed in the vicinity of the Southern Great Plains (SGP) Climate Research Facility operated by the U.S. Department of Energy (DOE) (Ackerman and Stokes 2003).

The location of the SGP site was chosen because it is representative of a large geographical area in the continental United States. This site is heavily instrumented for measurements of cloud, precipitation, radiation, and ambient meteorological parameters. The instrumentation deployed at this site in 2007 included surface precipitation gauges and ground-based radars operating at different frequencies, which allow independent estimates of precipitating cloud system parameters in the vertical atmospheric column above the SGP Central Facility (Matrosov 2009a,b). The availability of such SGP estimates presents an opportunity to compare ground-based retrievals with spaceborne *CloudSat* retrievals and conduct a consistency check for both remote sensing approaches.

2. Brief description of *CloudSat* retrieval approaches

The attenuation-based method for retrievals of rainfall parameters from CPR measurements (Matrosov 2007; Matrosov et al. 2008) was used to retrieve rain rates in the liquid hydrometeor layer along the *CloudSat* ground track. This method uses rainfall attenuation effects, which are strong at W band, as useful information. The vertical gradients of the observed reflectivity Z_e provide rain-rate estimates. These gradients are primarily shaped by attenuation, as nonattenuated rain reflectivities Z_{en} usually

change relatively little in comparison with changes due to attenuation (the changes in Z_{en} , however, contribute to the retrieval uncertainties).

The relative constancy of nonattenuated reflectivities in a vertical profile is especially true for stratiform rainfall, which usually exhibits only a 1–2-dB vertical variability in Z_{en} even for longer radar wavelengths (e.g., Bellon et al. 2005; Matrosov 2010). At shorter wavelengths, non-Rayleigh scattering effects further reduce this variability. In rainfall heavier than about 4 mm h^{-1} , these effects at W band are so strong that nonattenuated reflectivities do not exhibit any clear dependence on rain rate R , and they vary in a relatively narrow interval because of changes in rain drop size distributions (Matrosov 2007).

Estimates of the W-band rain attenuation coefficient α , obtained from the vertical gradients of observed reflectivity, are then related to rain rates using power-law α – R approximations. The attenuation contributions caused by the atmospheric gases (i.e., water vapor and oxygen) are accounted for by using a model profile of air density and assuming a 95% relative humidity in the rain layer. The attenuation contribution from the liquid water clouds is accounted for by assuming an average value of cloud liquid water path (LWP) ($\sim 400 \text{ g m}^{-2}$), which was estimated in stratiform rainfall conditions at the SGP site using the multifrequency radar measurements (Matrosov 2009b).

Multiple scattering (MS) effects present in *CloudSat* measurements cause an increase in the observed reflectivity values relative to those that would be measured in the event of single scattering (e.g., Battaglia et al. 2008). While these effects change the absolute values of observed reflectivities rather strongly, vertical gradients of the reflectivity in the rain layer are influenced to a much lesser extent. A correction procedure to account for MS effects in the attenuation-based reflectivity gradient method was recently suggested (Matrosov et al. 2008) for retrievals of rain rates that are less than about 20 mm h^{-1} . In heavier rains, MS effects usually overwhelm CPR returns. *CloudSat* precipitation retrievals are practically impossible for such rains using any remote sensing approach.

Very often CPR returns from precipitating cloud systems exhibit an obvious peak [i.e., bright band (BB)] in the melting region located just below a 0° isotherm. The physical mechanisms of this peak are somewhat different from the ones responsible for the radar bright bands usually observed at longer radar wavelengths (Sassen et al. 2007; Matrosov 2008). It is caused by an initial increase of radar returns from melting ice/snow particles (compared to dry ice/snow particles) followed by strong attenuation in the melting layer as radar signals further penetrate into this layer. The CPR BB signal can be used for separating the liquid and melting hydrometeor layers

from cloud parts dominated by ice. Attenuation of the radar signals in ice regions of the precipitating systems above the BB is usually much smaller than that in the liquid hydrometeor and melting layers, and radar reflectivities are dominated by the ice–snowflake particles. The BB features in *CloudSat* measurements are customarily seen in stratiform precipitation systems.

The ice water content (IWC) and its vertical integral ice water path (IWP) are estimated for cloud regions above the BB from observed reflectivity, using empirical IWC– Z_e relations. Although multiple scattering effects also enhance *CloudSat* reflectivities from these regions, this enhancement is small compared to that in rainfall and it is approximately balanced out by some modest attenuation caused by the ice particles. As a result, the CPR reflectivities observed above the BB in the areas outside convection regions might be considered a proxy to the single scattered nonattenuated reflectivities (Matrosov and Battaglia 2009), and appropriate IWC– Z_e relations can be used for ice phase retrievals. CPR-observed reflectivities of ice regions of precipitating cloud systems are usually very high (up to 20 dBZ or so). An IWC– Z_e relation specifically tailored for such regions and W-band measurements ($IWC = 0.086Z_e^{0.92}$, where IWC is in g m^{-3} and Z_e is in $\text{mm}^6 \text{m}^{-3}$) was recently suggested by Matrosov and Heymsfield (2008) who also compared this relation with other published relations. This relation accounts for nonsphericity of ice–snow particles and non-Rayleigh scattering effects. The rainfall and ice content retrieval remote sensing approaches outlined above were used in this study for estimating precipitating cloud parameters.

The advantage of *CloudSat* observations of the ice regions of precipitating cloud systems (compared to the ground-based cloud radar observations) is that satellite radar measurements experience little attenuation because of the viewing geometry and ice parts of these systems are vertically resolved in their entirety. For ground-based observations of precipitating cloud systems, radar measurements at additional frequencies are required to correct for strong attenuation in the intervening rainfall and melting layers (Matrosov 2009b) and, for heavier precipitation, the information from the regions near the cloud tops can be lost because of the total signal extinction.

3. Illustrations of the *CloudSat* observations and retrievals

Because of orbit parameters, the *CloudSat* satellite never passes directly over the SGP Atmospheric Radiation Measurement Program (ARM) Central Facility site where the vertically pointing cloud radars used for

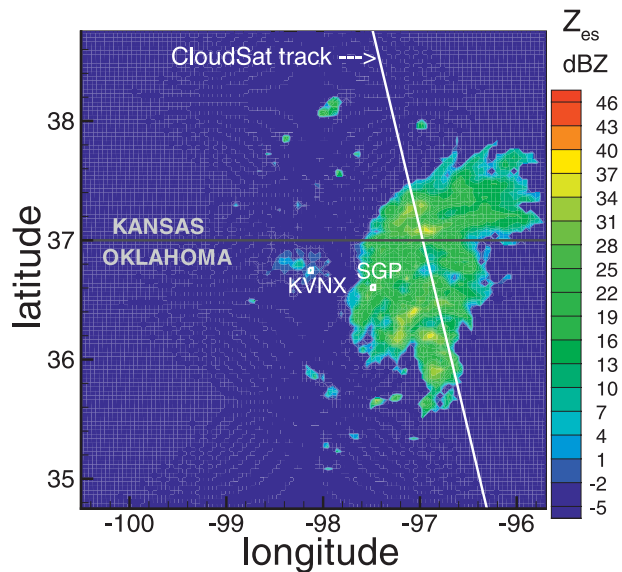


FIG. 1. WSR-88D KVNx radar view of a precipitation event around the SGP site on 27 May 2007 during the *CloudSat* overpass at 1947 UTC.

ground-based retrievals are located. The shortest horizontal separation of the CPR radar beam and the vertical column above the SGP Central Facility is about 56 km. During the period of *CloudSat* operations, only a few satellite overpasses happened when the same precipitating system was simultaneously observed by the DOE radars and *CloudSat* at this closest horizontal separation. One such overpass, which occurred on 27 May 2007 on the ascending orbit, is shown in Fig. 1. The *CloudSat* ground track in this figure is superimposed on the reflectivity map obtained with a 1.4° tilt from the scanning Weather Surveillance Radar-1988 Doppler (WSR-88D) operated at an S-band frequency for which attenuation is negligible. The National Weather Service 4-letter identifier for this radar is KVNx, and its location is also shown in Fig. 1. The vertical cross section of CPR reflectivity measurements corresponding to this *CloudSat* overpass is shown in Fig. 2. The freezing level height at an altitude of about 3.7 km above mean sea level (MSL) is manifested by the top of the BB. This height of the freezing level was also confirmed by the ground-based SGP measurements (not shown). Surface returns are seen in a layer located lower than about 0.6 km MSL.

a. Selection of *CloudSat* observations of precipitating cloud systems

Because of infrequent *CloudSat* overpasses when observing precipitating cloud systems in the immediate vicinity of the SGP site, consideration was given to all overpasses that occurred during the first three years of

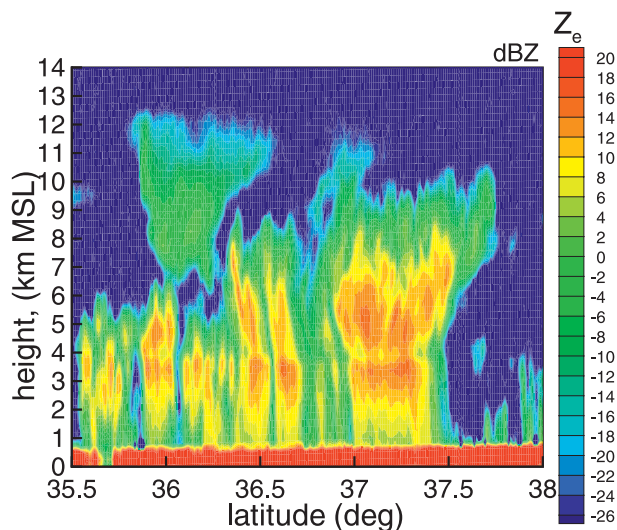


FIG. 2. The vertical cross section of *CloudSat* measurements during the SGP precipitation event observed on 27 May 2007.

CloudSat operations when CPR-observed precipitating cloud systems were within 500 km of the SGP site. Only stratiform precipitation cases were chosen for retrievals as they offer a relatively straightforward separation of the predominant water phase regions (i.e., ice, mixed, and liquid) by means of the radar bright band. The presence of this band in measurements is a convenient feature allowing classification of precipitation as stratiform (e.g., Houze 1993).

Figure 3 shows a cross section of *CloudSat* measurements in the vicinity of the SGP site on 28 August 2006. During the depicted overpass, two separate precipitating systems were observed in the selected 500-km range between the CPR radar beam and the SGP site. One of these systems observed between latitudes of 33.1° and 33.6° passed the criterion of being stratiform. The other system centered at latitude 34.5° was clearly convective. It had no BB features and the maximum radar reflectivities were observed well above the freezing level. In this study, the retrievals were not performed for convective events regardless of their distance from the SGP site.

An additional selection criterion for precipitation events chosen here for retrievals was that liquid hydrometeor layers be at least 1.5 km thick, so that sufficient attenuation of CPR signals occurred to allow rainfall retrievals, which are based on the attenuation effects. This criterion limited analyzed cases to relatively warm stratiform precipitation. Additionally, the horizontal ground track through the precipitation region, as observed by the CPR, needed to be at least 40 km to provide enough retrieval points for each event to be analyzed statistically. The total number of the SGP stratiform precipitation

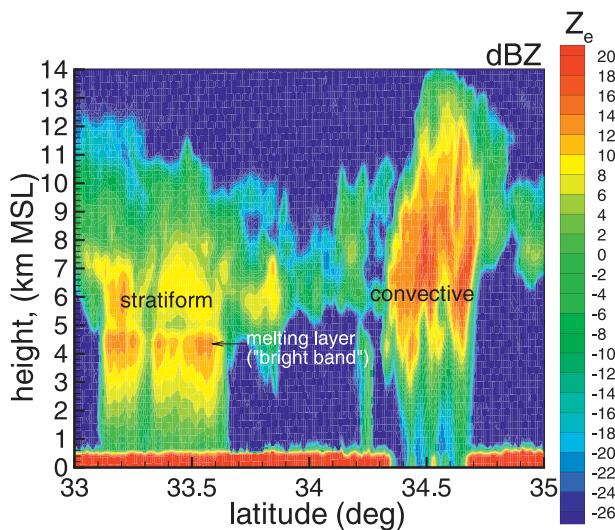


FIG. 3. The vertical cross section of *CloudSat* measurements during the SGP precipitation event observed on 28 Aug 2008. Stratiform and convective precipitation events are clearly identifiable.

events that qualified for *CloudSat* retrievals according to the criteria stated above was 14.

b. Examples of retrievals

The mean rain rate R_m and IWP were retrieved for each CPR vertical profile of measurements. Here R_m represents the mean value in a vertical layer that stretches from about 1 km below the top of the BB (i.e., below the melting layer) to about 1 km MSL. This choice of the rainfall retrieval layer boundaries is dictated by the need to avoid influences of partially melted ice/snow particles present in the melting layer, which usually is 0.5–0.7 km thick, and to rule out a contamination of *CloudSat* reflectivities by ground returns.

IWP values were obtained by vertically integrating IWC retrievals from the cloud echo top to the top of the BB. Profiles with retrieved $R_m < 0.5 \text{ mm h}^{-1}$ were not considered because of the high uncertainty of retrieving such light rainfall using the attenuation-based method (Matrosov 2007). Often the periods with retrieved values of $R_m < 0.5 \text{ mm h}^{-1}$ corresponded to CPR profiles with no clearly defined BB enhancements (e.g., regions between latitudes 36.7° and 37° in Fig. 2, and near latitude 33.3° in Fig. 3).

Figure 4 shows time series of the retrieved R_m and IWP for the stratiform precipitation events presented in Figs. 2 and 3. Gaps in the displayed data correspond to lighter rainfall with $R_m < 0.5 \text{ mm h}^{-1}$. For these events, the retrieved values of R_m are generally less than 4 mm h^{-1} and those of IWP vary from about 800 to 4000 g m^{-2} . Since the cloud-top heights generally exceeded 10 km MSL, large values of IWPs should not be

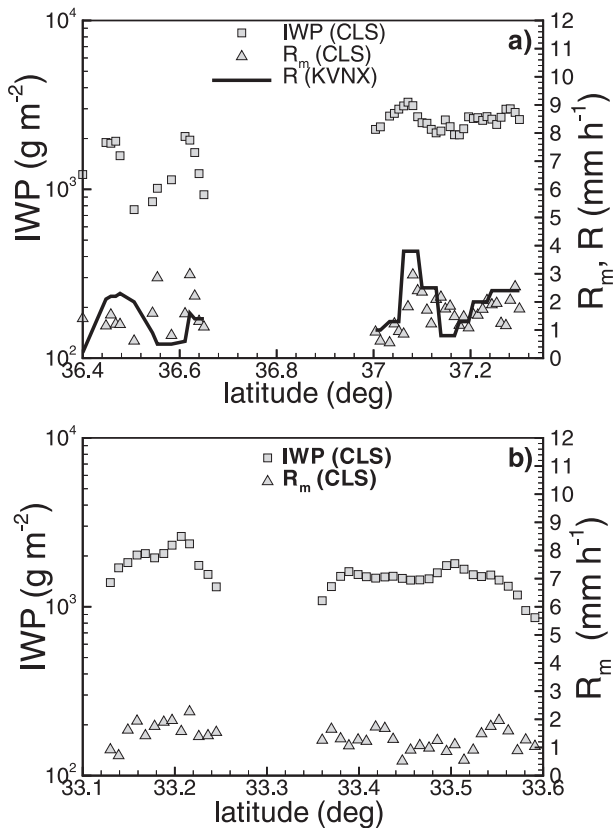


FIG. 4. The retrieved IWP (squares) and mean layer rain rate R_m (triangles) values for the stratiform precipitating systems observed by *CloudSat* on (a) 27 May 2007 and (b) 28 Aug 2008. Coincident KVN estimates are also shown in (a).

surprising given the large vertical extent of the high reflectivity ice regions of precipitating clouds.

Most of the ice mass in precipitating cloud systems is contained in regions of high reflectivity. Figure 5 shows the fraction of the total IWP that comes from cloud regions with observed reflectivities greater than 0 dBZ. It can be seen that this fraction is generally greater than 94%. It justifies the use of IWC– Z_e relations that are specifically tuned for such high reflectivities (Matrosov and Heymsfield 2008). Note also that using measurements from passive sensors aboard other satellites for combined retrievals of precipitating cloud systems over land is rather limited because of the high optical depth of the precipitating cloud systems and complexities resulting from the presence of ice, mixed, and liquid phases of water in the same vertical column. While the active measurements of *CloudSat* allow vertical separation of different phases, their individual contributions to passive measurements are difficult to quantify.

Figure 5 also presents the visible optical thickness retrievals of ice regions for the precipitating cloud systems

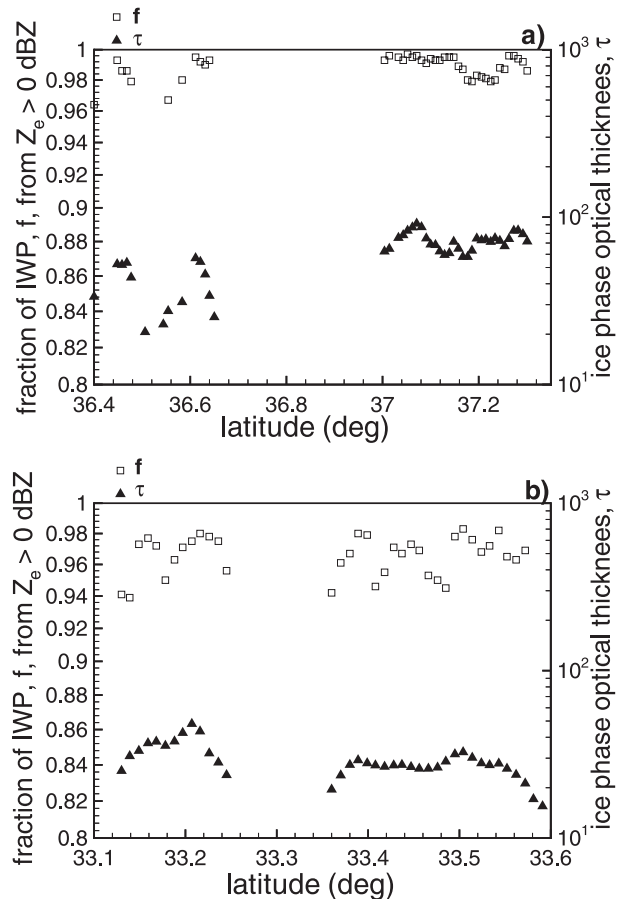


FIG. 5. The fraction of IWP from cloud parts with $Z_e > 0$ dBZ (squares) and ice region optical thicknesses (triangles) for the stratiform precipitating systems observed by *CloudSat* on (a) 27 May 2007 and (b) 28 Aug 2008.

shown in Figs. 2 and 3. The estimates of optical thickness τ , which is a vertical integral of the specific extinction, are based on a correspondence between W-band reflectivities and ice cloud particle cross sectional areas as inferred in a study by Matrosov and Heymsfield (2008). This correspondence results in a relation for the visible extinction coefficient α (m^{-1}) = $0.0014Z_e^{0.94}$ ($\text{mm}^6 \text{m}^{-3}$), which was used for the optical thickness estimates shown in Fig. 5. Both the extinction coefficient and IWC are approximately proportional to the second moment of the particle size distribution. IWC proportionality to the second moment of the size distribution is explained by the fact that effective particle density is typically proportional to the reciprocal of particle size (e.g., Matrosov et al. 2009). Because of this proportionality, the exponents in α – Z_e and IWC– Z_e relations are similar, which results in a close correspondence of minima and maxima locations of retrieved IWP and optical thickness values in Figs. 4 and 5.

For these events, the retrieved optical thickness values are generally between 20 and 100. These values present

estimates of τ due to contributions from just ice–snowflake particles. Nonprecipitating supercooled water drops, which might be present above the BB and are practically “invisible” to radar when coexisting in the radar resolution volume with much larger ice particles, may also contribute to the total visible extinction.

c. Retrieval uncertainties

The main sources of the attenuation-based *CloudSat* rain-rate retrieval uncertainties stem from variability of the relation between the attenuation coefficient at W band and the rain rate due to rain drop size distribution (DSD) changes as well as from the variability in nonattenuated reflectivity profile. It was estimated that the corresponding retrieval error can be as large as 35%–40% (Matrosov 2007). Additional uncertainties arise from the variability of the LWP of clouds that can coexist with rain in the liquid hydrometer layer, which is located between the base of the melting layer and the surface. Signal attenuation in clouds depends on LWP linearly. Ground-based multiwavelength radar retrievals indicate that a mean cloud LWP in the stratiform precipitation systems at the SGP site is about 400 g m^{-2} , and it does not significantly depend on the mean layer rain rate R_m (Matrosov 2009b). As mentioned previously, this mean value was assumed for the *CloudSat* retrievals in this study. For typical stratiform rain rates of $2\text{--}3 \text{ mm h}^{-1}$, a 200 g m^{-2} variability of the cloud LWP relative to this assumed mean value causes an additional uncertainty of about 15%–20% in the attenuation-based retrievals of rain rate. Assuming independence of this source of the total retrieval error and the error component caused by the DSD and nonattenuated reflectivity changes mentioned above, one can get a 40%–45% estimate for the total error of rain-rate retrieval (i.e., $0.35^2 + 0.15^2 \approx 0.40^2$ and $0.40^2 + 0.20^2 \approx 0.45^2$).

While the above estimate of the uncertainty in rain rates refers to individual values in a profile, it can be expected that estimates of the layer mean values R_m might have somewhat smaller uncertainties due to possible partial cancelations of errors as a result of vertical averaging. It should also be mentioned that the attenuation-based *CloudSat* retrievals of rain rate have been compared with results from surface-based precipitation radars. These comparisons showed the consistency of spaceborne attenuation-based retrievals, which typically agreed with surface-based precipitation radar estimates of rain rates within stated uncertainties (e.g., Matrosov 2007; Matrosov et al. 2008).

An important source of errors in radar estimates of ice content is the variability of the particle characteristic size (e.g., Atlas et al. 1995). Additional errors are caused by uncertainties in details of particle size distributions,

particle shapes, and reflectivity uncertainties. Relatively conservative estimates of radar reflectivity based retrieval errors of IWC (and hence of IWP) can be as high as a factor of 2 (e.g., Matrosov 2009b). This is not unusual for the radar reflectivity-based methods as comparisons of different ice cloud retrieval techniques indicate (Comstock et al. 2007). Note that these comparisons were performed for ice cloud layers observed without interfering liquid layers, so optical and passive measurement-based retrievals were also available for comparisons in addition to the radar-only results.

4. Relations between IWP and mean rain rate

Unlike for warm rain processes where interaction and conversion between cloud and rain liquid are crucial, ice/snowflake particle melting is the important mechanism for stratiform rainfall formation. Given this, a certain positive correlation between the total amount of ice observed above the melting layer and rainfall below this layer can be expected. The *CloudSat* simultaneous retrievals of IWP and R_m in stratiform precipitating systems described above can be used to assess this correlation from the observational data. Relations between IWP and R_m are sought in the power-law form:

$$\text{IWP} = aR_m^b, \quad (1)$$

because such a form is often used to describe the correspondence between different parameters in various parameterization schemes.

For the events shown in sections 2 and 3 as illustrations of *CloudSat* observations and retrievals, Fig. 6 depicts scatterplots between retrieved parameters and the corresponding best-fit power-law regression lines. While there is a moderate correlation between IWP and R_m for the event of 28 August 2006 (the corresponding correlation coefficient $r = 0.44$), the correlation coefficient for the event of 27 May 2007 is very low ($r = 0.17$). This later event is, however, of a particular interest because it was observed by *CloudSat* at the closest distance to the SGP site and happened during a relatively short instrument deployment period in 2007 (May–June 2007) when multiwavelength vertically pointing ARM cloud radar measurements were available at this site.

For comparisons with *CloudSat* rainfall retrievals during this event, KVNIX WSR-88D radar-based rain-rate estimates along the *CloudSat* track are also shown in Fig. 4a for areas where $R > 0.5 \text{ mm h}^{-1}$ and the KVNIX radar beam was entirely in the rain region. The default WSR-88D reflectivity–rainfall rate relation (i.e., $Z = 300R^{1.4}$ at S band) was used for these estimates. It

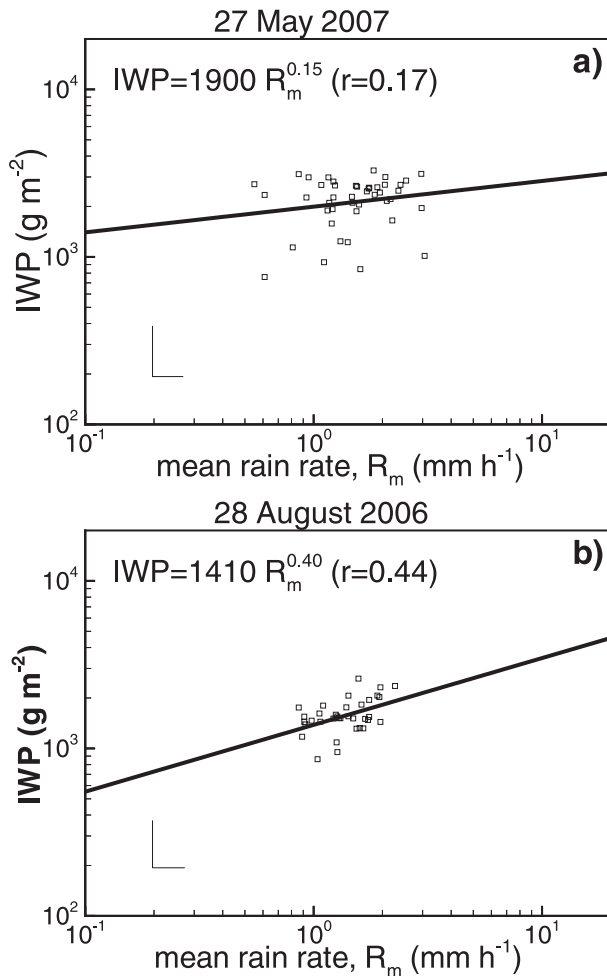


FIG. 6. Scatterplots of *CloudSat* retrievals of mean rain rate R_m and IWP for stratiform precipitation events observed on (a) 27 May 2007 and (b) 28 Aug 2006. The thin lines in the lower-left corner represent a factor of 2 (for IWP) and 40% (for R_m) error bars.

can be seen that the agreement between *CloudSat* and KVN_X rainfall data is very good for latitudes greater than 37°. While elsewhere the agreement is not that good, the difference between *CloudSat* and KVN_X estimates is generally within stated retrieval uncertainties (except a couple of data points).

Retrievals of the columnar values of IWP and R_m were available from the ground-based ARM radars for the 27 May 2007 event (Matrosov 2009b) for comparisons. Figure 7 shows scatterplots of *CloudSat* and ground-based radar retrievals. IWP and R_m values from both types of retrievals occupy approximately the same area in the IWP– R_m space. The mean values of IWP and R_m in Fig. 7 are 1460 g m⁻² and 1.4 mm h⁻¹ for ground-based retrievals and 2010 g m⁻² and 1.8 mm h⁻¹ for *CloudSat* retrievals. As with the satellite retrievals, the SGP estimates for this event also show no appreciable

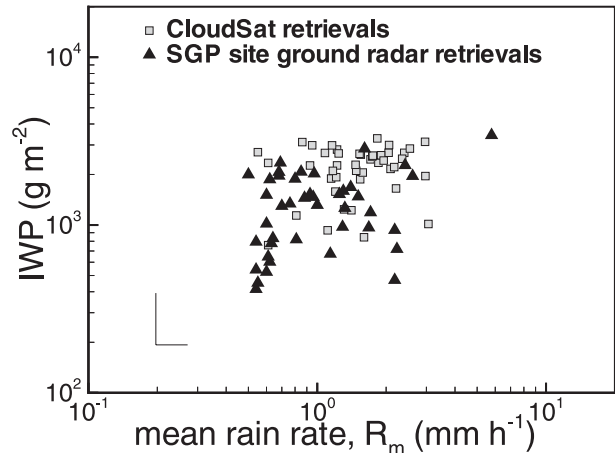


FIG. 7. Scatterplots of IWP–mean rain-rate retrievals from the SGP ground-based (triangles) and spaceborne *CloudSat* (squares) measurements for the event of 27 May 2007. The thin lines in the lower-left corner represent a factor of 2 (for IWP) and 40% (for R_m) error bars.

correlation between IWP and R_m with the correlation coefficient of only 0.03 (Matrosov 2009b). A direct point-by-point comparison cannot be performed for these two kinds of retrievals because the CPR and the vertically pointing cloud radars at the SGP site observe different volumes (though in the same precipitation cloud system). Nevertheless, the data in Fig. 7 indicate that ground-based and satellite retrievals of precipitating cloud parameters are mutually consistent within the stated uncertainties of the remote sensing methods.

Although the event of 27 May 2007 presents the smallest distance mismatch between *CloudSat* and ground-based estimates, the consistency between satellite and ground-based precipitating cloud parameter retrievals can be also checked using all 14 experimental events that were observed by *CloudSat* within the 500-km radius around the SGP ground site. Table 1 presents the best-fit power-law relations, sample sizes, and the corresponding correlation coefficients for these experimental events. As seen from the table, for the majority of the *CloudSat* experimental events, a moderate correlation (i.e., $0.3 < r < 0.7$) between IWP and R_m is present, but for a few cases the correlation coefficient is less than 0.3, which is typically regarded as low correlation. This generally agrees with the results of ground-based retrievals at the SGP site (Table 1 in Matrosov 2009b) where most of the stratiform precipitation events observed from the ground exhibited a moderate correlation between the retrieved values of IWP and R_m , and only for a couple of cases the correlation coefficient was less than 0.3 (including the 27 May 2007 event). Note that at sample sizes greater than 30, the estimates of correlation coefficients that exceed a value of about 0.3 are

TABLE 1. Parameters in the experimental $IWP = aR_m^b$ best-fit relations for the stratiform precipitating cloud events observed by *CloudSat* in the vicinity of the SGP site, sample sizes, and the corresponding power-law correlation coefficients (IWP : g m^{-2} ; R_m : mm h^{-1}).

Date of event	No.	a	b	r	Sample size
28 Aug 2006	1	1410	0.40	0.44	35
15 Oct 2006	2	3960	0.25	0.27	28
4 May 2007	3	4120	0.40	0.56	83
25 Apr 2007	4	3050	-0.02	0.18	14
27 May 2007	5	1900	0.15	0.17	45
28 Jun 2007	6	1240	0.28	0.30	80
8 Aug 2007	7	3480	0.33	0.54	56
24 Aug 2007	8	7410	0.14	0.37	158
6 May 2008	9	4220	0.41	0.41	166
23 Jun 2008	10	7780	0.11	0.47	27
13 Oct 2008	11	620	0.22	0.23	67
13 Mar 2008	12	4770	0.14	0.38	72
23 Apr 2008	13	4030	0.07	0.11	59
16 May 2008	14	1100	0.38	0.50	63

usually statistically significant at a 5% level. This level reflects a probability that the null hypothesis (i.e., no relation between parameters) is true (e.g., Borovkov 1997).

Figure 8 presents an IWP - R_m scatterplot for all 14 *CloudSat* observational events of stratiform precipitating cloud systems in the vicinity of the SGP site. The best-fit total integrated ice content-rainfall relation for this dataset is $IWP = 3060R_m^{0.36}$ and the total number of the retrieval points is 980. According to this relation, average changes of IWP over a typical interval of rain rates observed in stratiform precipitation (i.e., 0.5 – 12 mm h^{-1}) is a factor of about 3. This is greater than the expected uncertainty of IWP retrievals, which was estimated above rather conservatively as a factor of 2.

As seen from Fig. 8, the maximum values of *CloudSat* IWP retrievals in the precipitation cloud systems around the SGP site are around $10\,000 \text{ g m}^{-2}$. These values correspond to events when cloud tops were reaching altitudes of 14 km MSL or so (not shown). The lack of experimental data points with $IWPs$ significantly higher than $10\,000 \text{ g m}^{-2}$ is not likely to be due to “saturation effects” of W-band radar reflectivity measurements because similar highest IWP values were also retrieved from the ground with the combination of K_a - and S-band radars (Matrosov 2009b).

While there is a clear general trend of mean rain rate increasing with increased IWP , there are observational events with no clear trend (like the event of 27 May 2007 discussed in the previous section) and even events when R_m was increasing while IWP in the same vertical column was decreasing, which resulted in the exponent b in

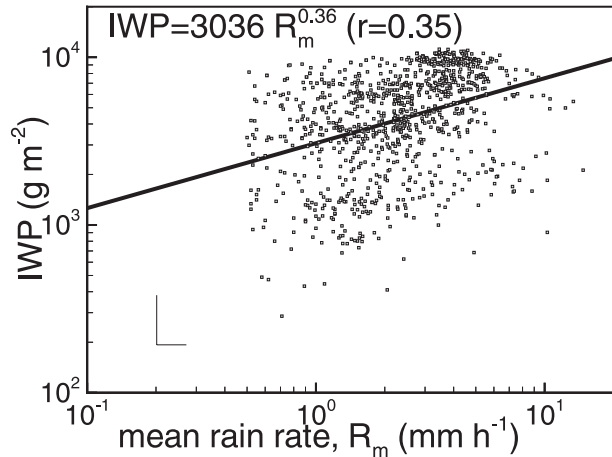


FIG. 8. The combined IWP - R_m scatterplot for stratiform precipitating cloud systems observed by *CloudSat* in the vicinity of the SGP site. The thin lines in the lower-left corner represent a factor of 2 (for IWP) and 40% (for R_m) error bars.

(1) being negative. Some similar “outlier” events were also observed using the ground-based multiwavelength radar approach at the SGP site (Matrosov 2009b). Without extensive modeling efforts, which are outside the scope of this study, it is difficult to speculate about the exact reasons of the negative correlation between IWP and R_m for a small number of the “outlier” events.

The mean *CloudSat* IWP - R_m relation shown for the data points in Fig. 8 agrees well with the best-fit relation obtained from the ground-based multiwavelength radar retrievals of May–June 2007 stratiform precipitation cases observed at the SGP Central Facility: $IWP = 2450R_m^{0.33}$ (Matrosov 2009b). Similar power-law correlation coefficients between IWP and R_m were also obtained (i.e., $r = 0.35$ for the satellite retrievals versus $r = 0.32$ for the ground-based retrievals). Such correlation coefficients correspond to the lower end of what is customarily considered as a range for moderate correlation (i.e., $0.3 < r < 0.7$). The mean values of retrieved parameters are similar for the *CloudSat* retrievals of this study ($IWP \approx 4900 \text{ g m}^{-2}$, $R_m \approx 2.8 \text{ mm h}^{-1}$) and the ground-based retrievals ($IWP \approx 4300 \text{ g m}^{-2}$, $R_m \approx 2.4 \text{ mm h}^{-1}$) from Matrosov (2009b). Note also that a similar correlation (~ 0.48) was found between cloud IWP and rain rate as inferred from Tropical Rainfall Measurement Mission (TRMM) data for oceanic events (Horváth and Davies 2007).

CloudSat data correspond to the cloud and rainfall parameters simultaneously retrieved in the same vertical column along the satellite track. Using surface-based measurements of the vertical profiles of horizontal winds at the SGP site, it was shown (Matrosov 2009b) that the vertical dependence of horizontal advection (i.e., wind

shear) causes decorrelation between IWP and R_m retrieved for the same vertical column from the vertically pointing ground-based cloud radars. Such decorrelation can also be expected for the *CloudSat* estimates, although it is difficult to assess it quantitatively in the framework of this study because of the lack of the high-resolution temporal and spatial wind information inside the precipitation systems sensed by the CPR.

Some possible manifestations of decorrelation effects can be qualitatively seen in Fig. 4a, which presents the *CloudSat* retrievals for the event of 27 May 2007. While the retrieval data for this event overall exhibit low correlation ($r = 0.17$), one can see the similarity of the IWP and R_m trends (at least for latitudes greater than 37°). The locations of maxima and minima in the R_m retrievals, however, are slightly shifted toward somewhat higher latitudes compared to the IWP retrievals. This shift might be caused by wind shear, which results in decorrelation of the IWP and R_m data.

Another factor that may influence the correlation between IWP and R_m is vertical air motion above the melting layer. Stronger upward motions would cause precipitation-sized ice particles to fall slower, which could result in higher ice mass centers and in some decorrelation. Detailed information on dynamical properties of precipitating systems (i.e., wind shear and vertical motions) is needed to better understand mechanisms influencing relations between ice contents of such systems and the resultant rainfall.

5. Conclusions

The measurements from *CloudSat*'s W-band nadir-pointing cloud-profiling radar (CPR) can be used to provide quantitative information about precipitating cloud systems. Because of its high sensitivity, the CPR is able to resolve vertical structures of these systems from ice cloud tops downward to the rain layers below. Absolute reflectivities in the rainfall layers are influenced by multiple scattering (MS) effects (because of a relatively large radar footprint) and attenuation. The MS effects, however, modify reflectivity gradients to a much lesser extent than their absolute values, and their impact on the gradients can be approximately corrected for; therefore, the attenuation-based gradient method, which does not rely on surface returns, can be used for estimations of rain rates. Thus *CloudSat* radar measurements provide an opportunity to quantitatively estimate rainfall in stratiform precipitating systems over land where other spaceborne sensors have certain problems because of highly variable surface emissivity and reflectance characteristics.

The ice regions of precipitating cloud systems are observed by the CPR without obstructing and strongly

attenuating intervening liquid layers, thus reflectivity-based estimators can be used for retrievals of cloud ice contents. Attenuation of CPR signals in cloud ice regions is small (compared to that by liquid and melting hydrometeors) and it is approximately balanced out by modest MS effects in these regions. Combining the reflectivity gradient-based approach for the rainfall layer and the absolute reflectivity-based estimators for the ice hydrometer layer retrievals can be used for high-spatial resolution and independent simultaneous-estimates of ice content and rainfall parameters in the same vertical atmospheric column; thus providing an opportunity for studying precipitation processes and elements of the global water cycle.

The combined retrieval approach was applied to stratiform precipitating cloud systems observed by the CPR in the vicinity of the SGP ground-based instrumented site during the first three years of *CloudSat* operations. The stratiform precipitating systems exhibit brightband features, which are identifiable in CPR reflectivity measurements. These features are caused by increased backscattering and attenuation of radar signals by melting ice and snowflake particles, and they allow separating among predominant hydrometer phases (i.e., ice, mixed and liquid) in a vertical profile as resolved by the CPR measurements.

The *CloudSat* retrievals of the mean layer rain rate R_m and ice water path (IWP) revealed the range of variability in IWP from a few 100s of g m^{-2} to about 10^4 g m^{-2} while R_m was varying from 0.5 mm h^{-1} (lower rain rates were not considered because of higher retrieval uncertainties) to about $10\text{--}12 \text{ mm h}^{-1}$. For typical observational events, CPR-based estimates of visible optical thickness of ice regions of precipitating cloud systems generally varied from 20 to 100. The independently retrieved values of IWP and R_m , as estimated simultaneously for the same vertical column, exhibited, on average, a moderate correlation. The mean correlation coefficient, however, was 0.35 while the coefficients for individual observational events varied from about 0.1 to 0.56. Horizontal advection, wind shear, and vertical air motions can cause decorrelation of the columnar values of IWP and R_m , which might be a reason for a lack of appreciable correlation between these parameters in some observational cases.

CloudSat retrievals of IWP and mean rain rate were compared with ground-based estimates of these parameters from the multiwavelength radar measurements at the SGP Central Facility during the May–June period of 2007. These comparisons indicated a general consistency between results of spaceborne and ground-based retrieval results, which was manifested in similar mean IWP– R_m relations and in similar variability ranges for both total ice content and rain-rate retrievals. Although

the ground-based and satellite measurements are not coincident and this comparison cannot be regarded as a strict validation effort, the general consistency is reassuring because both retrieval approaches use independent measurements. Future comparisons of *CloudSat* and ground-based retrievals of parameters of precipitating cloud systems could be available when a suite of new cloud radars will be deployed at the ARM facility.

Acknowledgments. This study was funded through NASA Project NNX07AQ82G and through the Office of Science, U.S. Department of Energy Grant DE-FG02-05ER63954.

REFERENCES

- Ackerman, T. P., and G. Stokes, 2003: The Atmospheric Radiation Measurement Program. *Phys. Today*, **56**, 38–45.
- Atlas, D., S. Y. Matrosov, A. J. Heymsfield, M. D. Chou, and D. B. Wolf, 1995: Radar and radiation properties of ice clouds. *J. Appl. Meteor.*, **34**, 2329–2345.
- Battaglia, A., S. Kobayashi, S. Tanelli, C. Simmer, and E. Im, 2008: Multiple scattering effects in pulsed radar systems: An inter-comparison study. *J. Atmos. Oceanic Technol.*, **25**, 1556–1567.
- Bellon, A., G. W. Lee, and I. Zawadzki, 2005: Error statistics in VPR corrections in stratiform precipitation. *J. Appl. Meteor.*, **44**, 998–1015.
- Borovkov, A. A., 1997: *Mathematical Statistics*. Nauka, 772 pp.
- Comstock, J. M., and Coauthors, 2007: An intercomparison of microphysical retrieval algorithms for upper-tropospheric ice clouds. *Bull. Amer. Meteor. Soc.*, **88**, 191–204.
- Durden, S. L., S. Tanelli, and G. Dobrowalski, 2009: CloudSat and A-Train observations of tropical cyclones. *Open Atmos. Sci. J.*, **3**, 80–92.
- Haynes, J. M., T. S. L'Ecuyer, G. L. Stephens, S. D. Miller, C. Mitrescu, N. B. Wood, and S. Tanelli, 2009: Rainfall retrieval over the ocean with spaceborne W-band radar. *J. Geophys. Res.*, **114**, D00A22, doi:10.1029/2008JD009973.
- Horváth, Á., and R. Davies, 2007: Comparison of microwave and optical cloud water path estimates from TMI, MODIS, and MISR. *J. Geophys. Res.*, **112**, D01202, doi:10.1029/2006JD007101.
- Houze, R. A., Jr., 1993: *Cloud Dynamics*. Academic Press, 570 pp.
- Matrosov, S. Y., 2007: Potential for attenuation-based estimations of rainfall rate from CloudSat. *Geophys. Res. Lett.*, **34**, L05817, doi:10.1029/2006GL029161.
- , 2008: Assessment of radar signal attenuation caused by the melting hydrometeor layer. *IEEE Trans. Geosci. Remote Sens.*, **46**, 1039–1047.
- , 2009a: A method to estimate vertically integrated amounts of cloud ice and liquid and mean rate in stratiform precipitation from radar and auxiliary data. *J. Appl. Meteor. Climatol.*, **48**, 1398–1410.
- , 2009b: Simultaneous estimates of cloud and rainfall parameters in the atmospheric vertical column above the Atmospheric Radiation Measurement Program southern Great Plains site. *J. Geophys. Res.*, **114**, D22201, doi:10.1029/2009JD012004.
- , 2010: Synergetic use of millimeter- and centimeter-wavelength radars for retrievals of cloud and rainfall parameters. *Atmos. Chem. Phys.*, **10**, 3321–3331.
- , and A. J. Heymsfield, 2008: Estimating ice content and extinction in precipitating cloud systems from CloudSat radar measurements. *J. Geophys. Res.*, **113**, D00A05, doi:10.1029/2007JD009633.
- , and A. Battaglia, 2009: Influence of multiple scattering on CloudSat measurements in snow: A model study. *Geophys. Res. Lett.*, **36**, L12806, doi:10.1029/2009GL038704.
- , —, and P. Rodriguez, 2008: Effects of multiple scattering on attenuation-based retrievals of stratiform rainfall from CloudSat. *J. Atmos. Oceanic Technol.*, **25**, 2199–2208.
- , C. Campbell, D. Kingsmill, and E. Sukovich, 2009: Assessing snowfall rates from X-band radar reflectivity measurements. *J. Atmos. Oceanic Technol.*, **26**, 2324–2339.
- Sassen, K., S. Y. Matrosov, and J. Campbell, 2007: CloudSat spaceborne 94 GHz radar bright bands in the melting layer: An attenuation-driven upside-down lidar analog. *Geophys. Res. Lett.*, **34**, L16818, doi:10.1029/2007GL030291.
- Stephens, G. L., and Coauthors, 2008: CloudSat mission: Performance and early science after the first year of operation. *J. Geophys. Res.*, **113**, D00A18, doi:10.1029/2008JD009982.
- Tanelli, S., S. L. Durden, E. Im, K. S. Pak, D. Reinke, P. Partain, R. Marchand, and J. Haynes, 2008: CloudSat's cloud profiling radar after 2 years in orbit: Performance, external calibration, and processing. *IEEE Trans. Geosci. Remote Sens.*, **46**, 3560–3573.